# Temperature-dependent Analytical Thermal Model for End-pumped Solid-state Lasers

**Luigi Cini[1,3] , Wendell O.S. Bailey[2], Yifeng Yang[2], and Jacob I. Mackenzie[3]**
[1] *Dipartimento di Fisica, Università di Pisa, Largo B. Pontecorvo 3, Pisa, 56127, Italy*
[2] *Institute of Cryogenics, University of Southampton, SO17 1BJ, UK*
[3] *Optoelectronics Research Centre, University of Southampton, SO17 1BJ, UK*
J.I.Mackenzie@soton.ac.uk

**Abstract:** Analytical expressions for the temperature distribution and thermal-lens power in end-pumped solid-state lasers are reported. Enabled by including a temperature-dependent thermal conductivity, applicable from cryogenic to elevated temperatures, these prove insightful for practical systems.
**OCIS codes:** (140.6810) Thermal effects; (140.3430) Laser theory; (140.3380) Laser materials.

## 1. Introduction

As a mature laser architecture, the end-pumped solid-state laser is exploited for many scientific, industrial and medical laser applications in the tens-of-watts power regime. The basic power-scaling design strategy for these lasers has been to mitigate the effects of the induced thermal lensing and aberrations [1]. As such it is important to understand, and have effective tools to model, the induced temperature distribution over the active volume of interest. Typically, this involves numerical simulations solving the heat conductance equation using finite element algorithms, which in the age of powerful computing have almost completely replaced analytical solutions. Nevertheless, the importance of analytical solutions is unquestionable: as they provide insight into qualitative and quantitative features of underlying physical phenomena, and, accurate solutions in far less time than numerical calculations, particularly important when trying to perform parameter-dependence studies. In this paper we will present a series of simple analytical solutions to the non-linear heat conductance equation, derived via the inclusion of a temperature-dependent thermal conductivity and the use of the Kirchoff integral transform. This converts the problem into a solvable linear equation applicable to radially-isotropic cylindrical laser rods, and a vast range of potential operating temperatures. Four practical end-pumping-distributions are discussed and the resulting temperature profiles in the laser rod presented for each, which are then compared with exemplar temperature-independent expressions from literature.

## 2. Theory

Writing the steady state heat conductance equation, with temperature-dependent thermal conductivity, $k(T)$, and a heat source $S(r,z)$, we have:

$$\boldsymbol{\nabla} \cdot [k(T)\boldsymbol{\nabla}\mathrm{T}(r,z)] + S(r,z) = 0$$

We use a definition for thermal conductivity, $k(T) = k_0 \left(\frac{T}{T_0}\right)^m$

where $k_0$is the thermal conductivity at a reference temperature $T_0$, with the index $m$ providing the power dependence for the thermal conductivity on temperature. Typically, as shown later at least two values of $m$ are required to cover the cryogenic or elevated temperature ranges.

Using the Kirchhoff transform, $U(r,z) = \int^T k(\tau)d\tau$

gives $U = \frac{k_0}{T_0^m(m+1)} T^{m+1} + C,$

with an arbitrary constant $C$,

then the heat equation becomes: $\nabla U(r,z) = \frac{1}{r}\frac{dU(r,z)}{dr} + \frac{d^2U(r,z)}{dr^2} = -S(r,z),$

a solvable equation for various pumping distributions that define the heat source $S(r,z)$.

The resulting temperature profiles for two extreme pumping distributions, Gaussian (G) and top-hat (TH) are:

$$\mathrm{T}_G(r,z) = \left\{\frac{\eta_h P_{in}\alpha e^{-\alpha z}(m+1)T_0^m}{4\pi k_0}\left[ln\left(\frac{b^2}{r^2}\right) + E_i\left(\frac{2b^2}{\omega^2}\right) - E_i\left(\frac{2r^2}{\omega^2}\right)\right] + \left[T_c + \frac{\eta_h P_{in}\alpha e^{-\alpha z}}{2\pi bh}\right]^{m+1}\right\}^{\frac{1}{m+1}}$$

$$T_{TH1}(r,z)=\left\{\frac{\eta_h P_{in}\alpha e^{-\alpha z}(m+1)T_0^m}{4\pi k_0}\left[1-\frac{r^2}{a^2}+ln\left(\frac{b^2}{a^2}\right)\right]+\left[T_c+\frac{\eta_h P_{in}\alpha e^{-\alpha z}}{2\pi bh}\right]^{m+1}\right\}^{\frac{1}{m+1}},0\le r\le a$$

$$T_{TH2}(r,z)=\left\{\frac{\eta_h P_{in}\alpha e^{-\alpha z}(m+1)T_0^m}{4\pi k_0}ln\left(\frac{b^2}{a^2}\right)+\left[T_c+\frac{\eta_h P_{in}\alpha e^{-\alpha z}}{2\pi bh}\right]^{m+1}\right\}^{\frac{1}{m+1}},a\le r\le b$$

Where the new parameters in these equations are: $\eta_h$, the fractional thermal load for the incident power, $P_{in}$, which has an absorption coefficient $\alpha$, in a rod of radius $b$, and a thermal conductance at its boundary of $h$, and finally $E_i$, is the exponential integral function. The respective pump beams are assumed to have beam radii of $\omega$ and $a$. For the top-hat pump, the temperature profile has two different solutions whether inside, $T_{TH1}$, or outside, $T_{TH2}$, the excitation volume. Under the typical assumption of a constant $k_0$, when $m=0$, these equations are equivalent to those reported by Innocenzi [2] and Cousins [3].

### 3. Results and discussion

We have measured the thermal conductivity of 1.3at.% Nd:YAG in the cryogenic regime, and using the data reported in [4] at and above room temperature for a 1.2at.% doping, we find a good fit over two regions; CT 40 K≤ T≤175 K and RT 300 K≤ T≤475K, with the respective parameters, $m_{CT}=-1.77$ and $m_{RT}=-0.75$, for the intersection point at $T_0=164.17\ K$, with $k_0=15.09\ W/m.K$, as shown in Fig. 1a. In Fig. 1b, four different pumping distributions are represented, starting with a top-hat, Gaussian, a first-order approximation for a super-Gaussian, and an annulus (donut). Typical parameters for a diode-end-pumped rod laser are chosen, such that the rod has a 5 mm length ($L$) and 2.5 mm diameter, a pump-beam radii of 300 μm, $\eta_h=0.25$ and an incident power of 25 W with an $\alpha=350$ m$^{-1}$.

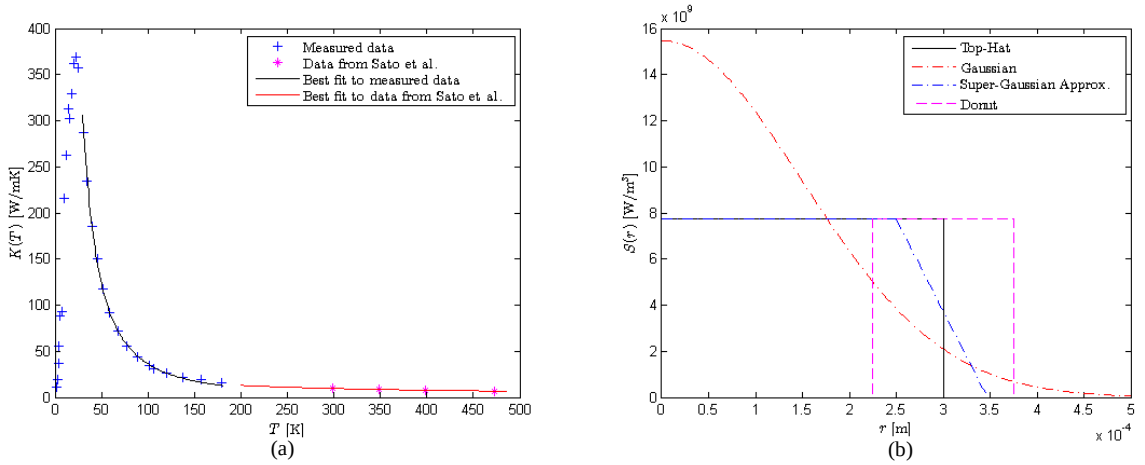


Fig. 1.a) Measured thermal conductivity of Nd:YAG as a function of temperature, in the CT and RT [4] regimes.b) four pump distributions investigated.

Temperature profiles at the input facet of the rod are shown in Fig. 2(a) for each of the corresponding pump distributions. It is clear that the Gaussian has the highest on axis temperature rise, associated with its higher power density Fig. 1(b). Furthermore, considering the TH pump, the temperature profile between the edge of the rod and the center are shown for several heat sink temperatures across the CT and RT ranges, highlighting the benefit of cryogenic cooling the crystal with increased thermal conductivity, Fig. 2(b). An additional advantage of these analytical solutions is that the dependence of the rod-center temperature on the boundary thermal conductance, h, is inherently part of the solution, as pointed out by [5]. This brings to the fore an important fact that was missing from previous solutions, [2], which were independent of h, and for which there is a critical value, below this value the rod temperature increases dramatically, Fig. 3(a).

Armed with the temperature gradients in the laser rod, it is a straightforward matter to obtain equations describing the induced parabolic thermal-lens power dependent upon the resulting optical path difference between on- and off-axis rays influenced by the thermo-optic coefficient. The thermal-lens dioptric power is found to be:

$$D_{th}=\frac{4\chi}{A\alpha B}\left\{\left[\frac{\eta_h P_{in}\alpha(m+1)T_0^m}{4\pi k_0}(B)+T_c^{m+1}\right]^{\frac{1}{m+1}}-\left[\frac{\eta_h P_{in}\alpha(m+1)T_0^m}{4\pi k_0}(B)e^{-\alpha L}+T_c^{m+1}\right]^{\frac{1}{m+1}}\right\}$$

Where for a Gaussian $A=\omega^2\ and\ B=\gamma+ln\left(\frac{2b^2}{A}\right)$; while for a TH $A=2a^2\ and\ B=1+ln\left(\frac{2b^2}{A}\right)$.

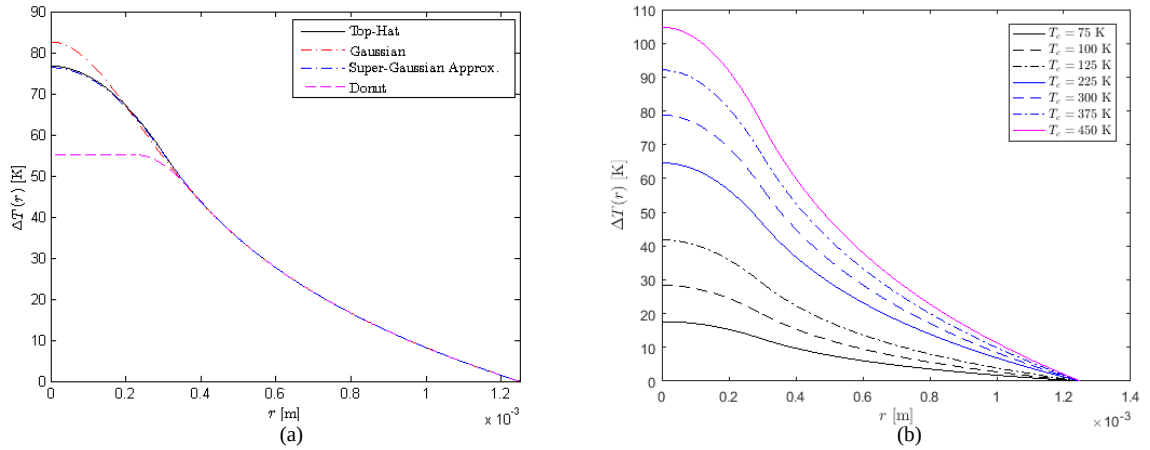


(a) (b)

Fig 2(a) Temperature profiles at the input facet of the rod for the four pump distributions; (b) temperature difference at the rod pump-input face, with respect to the rod-surface for a TH pump distribution, as detailed above, at various heat sink temperatures across the CT and RT ranges.

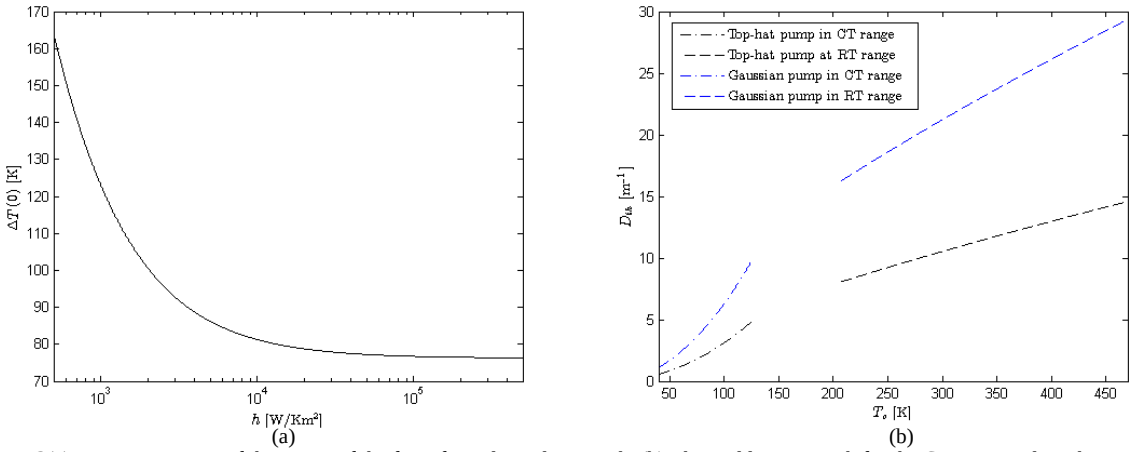


(a) (b)

Fig 3(a) Temperature rise of the center of the front facet dependence on h. (b) Thermal lens strength for the Gaussian and top-hat pump distributions as a function of heat-sink temperature.

For Fig. 3(b) the truncated calculation is due to the fit curve not covering the central temperature region and the deviation towards the ends of each region leads to a discontinuous result. Including a third fitting function across this region would solve this break in the data. Nonetheless it is apparent that the rate in change in thermal lens strength reduces with elevated temperatures, even if significantly stronger than at CT.

## 4. Conclusions

Key analytical expressions for the temperature profiles in end-pumped lasers are derived. These equations provide unique and expedient solutions for determining the expected temperature rise associated with a particular pumping distribution (top-hat, Gaussian, quasi-super Gaussian and annular). Critical dependence upon the boundary thermal conductance is described and highlights that the quality of the thermal interface sets a limit to the thermal load that can be generated in the rod. These equations will simplify the laser designers' toolbox and decrease the time needed to predict the end-pumped bulk lasers thermal characteristics over a range of coolant temperatures.

## 5. References

[1] W. A. Clarkson, "Thermal effects and their mitigation in end-pumped solid-state lasers," J. Phys. D-Appl. Phys. **34**, 2381-2395 (2001).
[2] M. E. Innocenzi, H. T. Yura, C. L. Fincher, and R. A. Fields, "Thermal modeling of continuous-wave end-pumped solids-state lasers," Appl. Phys. Lett. **56**, 1831-1833 (1990).
[3] A. K. Cousins, "Temperature and thermal-stress scaling in finite-length end-pumped laser rods " IEEE J. Quantum Electron. **28**, 1057-1069 (1992).
[4] Y. Sato, J. Akiyama, and T. Taira, "Effects of rare-earth doping on thermal conductivity in Y3Al5O12 crystals," Opt. Mater. **31**, 720-724 (2009).
[5] S. Chenais, F. Druon, S. Forget, F. Balembois, and P. Georges, "On thermal effects in solid-state lasers: The case of ytterbium-doped materials," Prog. Quantum Electron. **30**, 89-153 (2006).